

Yarn-Level Cloth Simulation with Sliding Persistent Contacts

Gabriel Cirio, Jorge Lopez-Moreno, and Miguel A. Otaduy

Abstract—Cloth is made of yarns that are stitched together forming semi-regular patterns. Due to the complexity of stitches and patterns, the macroscopic behavior of cloth is dictated by the contact interactions between yarns, not by the mechanical properties of yarns alone. The computation of cloth mechanics at the yarn level appears as a computationally complex and costly process at first sight, due to the need to resolve many fine-scale contact interactions. We propose instead an efficient representation of cloth at the yarn level that treats yarn-yarn contacts as persistent, but with the possibility to slide, thereby avoiding expensive contact handling altogether. We introduce a compact representation of yarn geometry and kinematics, capturing the essential deformation modes of yarn crossings, loops, stitches, and stacks, with a minimum cost. Based on this representation, we design force models that reproduce the characteristic macroscopic behavior of yarn-based fabrics. Our approach is suited for both woven and knitted fabrics. We demonstrate the efficiency of our method on simulations with millions of degrees of freedom (hundreds of thousands of yarn loops), almost one order of magnitude faster than previous techniques. We also compare the different macroscopic behavior under woven and knitted patterns with the same yarn density.

Index Terms—Yarns, Knitted cloth, Woven cloth, Physically based simulation.

1 INTRODUCTION

THE vast majority of garments are made of a yarn structure, either knitted or woven, and the macroscopic behavior of cloth is dictated by the mechanical interactions taking place at the yarn level. However, most cloth simulation models in computer graphics ignore the relevance of such yarn structure, represent the cloth surface as an arbitrary mesh, and compute internal elastic forces either by discretizing continuum elasticity models [1] or using discrete elastic elements [2], [3].

The seminal work of Kaldor et al. [4] proposed an alternative approach for knitted cloth, describing individual yarns using a rod model, and resolving contact interactions between yarns. A yarn-based model enables the simulation of complex small-scale effects, such as yarn-yarn friction and sliding, snags, pulls, frayed edges, or detailed fracture. Yet Kaldor et al. also showed that, with a yarn-based model, the macroscopic nonlinear mechanics of garments arise naturally through aggregation of yarn-level structural effects. But their method is hindered by a major challenge: efficient and robust detection and resolution of all yarn contacts. They later improved performance by reusing linearized contact information whenever possible [5].

In recent work, Cirio et al. introduced a novel representation of yarn-yarn interactions as persistent contacts with yarn sliding. With this representation, they achieved robust and efficient simulations, as they avoided the detection and resolution of yarn-yarn contacts altogether. The representation based on persistent contacts has been demonstrated on woven cloth [6] and limited types of knitted cloth [7]. In this work, we generalize this representation to handle more diverse types of knitted cloth, with complex stitches

formed by multiple yarns. All types of cloth, both woven and knitted, can be simulated under the same framework.

For woven cloth, we place one persistent contact node at each crossing of weft and warp yarns. For knitted cloth, we place two persistent contact nodes at the end points of each stitch contact. In this work, we augment the representation for knit stitches, supporting stitches with multiple yarns. Each persistent contact node is shared by several stacked yarns, and each yarn contributes one sliding coordinate. This choice of discretization is compact, yet it succeeds to capture yarn-level deformation modes that produce relevant macroscopic nonlinearities.

We inherit the derivation of the dynamics equations and the simulation algorithm from the original formulation for woven cloth [6]; therefore, we leave those aspects out in this paper. In spite of the algorithmic similarities, there are fundamental structural differences in the arrangement of yarns in woven and knitted cloth, which produce different inter-yarn contact mechanics. We have designed force models for yarn bending and stitch wrapping in knitted fabrics. In this paper, we introduce an algorithm to estimate compression forces at persistent contacts, which seamlessly handles persistent contacts with an arbitrary number of stacked yarns. Based on such compressive forces, we also introduce in this paper a model of sliding friction for multi-yarn persistent contacts. We have carried out experiments that evaluate the influence of yarn-level mechanical and geometric parameters on macroscopic mechanical behavior, and we observe the characteristic stretch, shear, and bending behavior of knitted fabrics, with manifest anisotropy, nonlinear stretch behavior, and plasticity.

We demonstrate the application of our yarn-level fabric representation to diverse types of knitting patterns, with both simple and complex stitches. On garments of similar complexity to those simulated by Kaldor et al. [5], such as

• G. Cirio, J. Lopez-Moreno, and M. A. Otaduy are with Universidad Rey Juan Carlos, Madrid.



Fig. 1. Yarn-level simulation of a knitted sweater with 56K loops (220K contact nodes, 1.1M DoFs), computed at 1.5 minutes per frame. Our model captures robustly and efficiently both the fine- and large-scale mechanics of knitted cloth.

the sweater shown in Fig. 1, with over 56K stitch loops, we achieve a 7 \times speed-up (without accounting for hardware differences). But with our method we are also able to simulate much denser fabrics, up to common real-world gauges, such as the shirt in Fig. 10, with 325K loops.

2 RELATED WORK

Yarn-level models of knitted and woven fabrics have a long history, dating back to 1937 when Peirce [8] proposed a geometric model to represent the crossing of yarns in woven fabric. Yarn-level models have been thoroughly studied in the field of textile research, initially using analytical yarn models [9] to predict the mechanical behavior of fabric under specific modes of deformation [8], [10]. Later, textile research relied on continuum models to simulate most yarn deformation modes and complex yarn-yarn contact interactions [11], [12], [13]. A number of techniques have been developed to alleviate the large computational burden of yarn-level continuum models, such as using multiscale models that resort to costly yarn-level mechanics only when needed [14], or replacing the complex volumetric yarns by simpler elements such as beams, trusses and membranes [15], [16].

Knitted fabric has received less attention compared to woven, perhaps due to the higher geometric complexity, which leads to more involved yarn contact interactions. Splines are often used to efficiently represent knit yarns, as introduced by Remion et al. [17]. Splines have also been used to approximate woven fabric in a purely geometric way (see e.g., [18], [19]), sometimes combined with thin sheet models in a multiscale fashion [20].

Often, yarn-level models capture the most relevant deformations and yarn interactions using specialized force models, such as bending and crossover springs to capture cross-sectional deformation and shear at crossover points [21], [22], truss elements acting as contact forces between yarns to capture shear jamming [21], or a slip velocity to capture yarn sliding [23]. As a consequence, these models enable the simulation of realistic macroscopic behaviors of fabric. However, yarn-level models in textile research focus on small portions of fabric, often in controlled experiments, and cannot simulate entire garments under free motions, nor single-yarn plastic effects such as snags, pulls and pullouts.

Recently, yarn-level models that address these shortcomings have emerged in the field of computer graphics. The seminal work of Kaldor et al. [4] was the first approach capable of simulating entire garments at the yarn level in tractable time, from loose scarves and leg warmers to large sweaters. Focusing on knits, they modeled the mechanics of individual yarns using inextensible rods, and computed yarn-yarn contact through stiff penalty forces and velocity-filter friction, allowing them to predict the large-scale behavior of full garments from fundamental yarn mechanics. They extended their work by using local rotated linearizations of penalty forces to accelerate yarn-yarn contact handling [5]. Yuksel et al. [24], on the other hand, designed geometric methods to create simulation-ready yarn-level models of many knit patterns.

Cirio et al. proposed a different approach, initially for woven cloth [6]. They assumed that yarn-yarn contacts are persistent in time, even under moderately large plastic deformations. This assumption avoids the need for expensive yarn-yarn collision detection and contact handling, thus greatly reducing simulation costs. They simulated every yarn in the fabric as a flexible rod, and introduced additional sliding degrees of freedom at yarn crossings to allow yarns to slide along each other and thus generate complex plastic effects such as snags, pulls, fracture and frayed edges. Other yarn-level models (mainly geometric and analytical ones) also assumed persistent contact, but they did not incorporate sliding coordinates.

More recently, they leveraged the concept of persistent contact with sliding degrees of freedom and extended it to the other large family of fabrics, knitted cloth [7]. Contacts in knitted fabric are more complex than in woven, hence it is not sufficient to represent each contact as one crossing node with sliding coordinates. Through observation of the deformation modes present in knit loops, they concluded that representing each stitch contact using two persistent contacts with yarn sliding on its end points would suffice to capture all the interesting deformation modes. This approach leads to a much more compact and efficient representation than previous work for knitted cloth, while still enabling all yarn-level interactions that produce interesting and realistic small- and large-scale behaviors. In this paper, we extend the previous work of Cirio et al. on knitted cloth to handle more complex stitches, and devise a formulation that is general to many woven and knitted fabrics. We

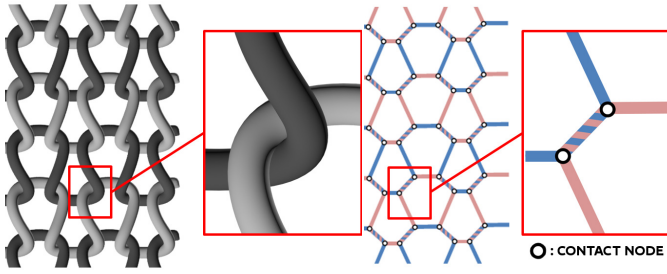


Fig. 2. Images of a simple stockinette knit and its discretization. From left to right: loops of a knit in 3D, zoom on a stitch in 3D, discretization of the knit, and zoom on a discretized stitch with two persistent contacts.

also design force models for complex stitches involving an arbitrary number of stacked yarns.

Sueda et al. [25] introduced a general formulation of Lagrangian mechanics to simulate efficiently the dynamics of highly constrained rods, through an optimal set of generalized coordinates that combine absolute motion with sliding on constraint manifolds. We apply this formulation to stacks of yarns with sliding persistent contacts.

3 YARN DISCRETIZATION

We begin this section by describing the yarn-based structure of fabrics, both woven and knitted, with a focus on the influence of this structure on the macroscopic behavior of garments. Understanding the yarn-based structure and its effects is important because it defines the requirements for our model, and it also anticipates many of its insights. Then, we continue the section by presenting our central idea, a representation of yarn-based cloth using persistent contacts. This representation is compact, yet it aims to capture the mechanically relevant characteristics of the yarn structure. We also discuss specifics of the application of persistent contacts for the representation of woven fabrics, simple knitted fabrics, and complex knitted fabrics.

3.1 Structure of Yarn-Based Fabrics

Both woven and knitted cloth are designed by setting up a network of yarns, interlaced or stitched. In woven cloth, typically two sets of orthogonal yarns, called warp and weft, are interlaced. Interlaced yarns undergo friction forces at yarn-yarn contacts, and this friction holds together the woven fabric. A *float* constitutes a gap between two yarns of the same type where the other yarn is not interlaced. Different weave patterns, such as plain weave (with no floats), twill, satin, etc. are obtained by varying the distribution of floats, thereby affecting the mechanics of the resulting fabric. Please see [6] for a detailed description of the construction of yarn-based models of woven cloth.

In knitted cloth, a single yarn is laid out in a chain of loops along a row of the so-called *course* direction. In simple knits, these loops are pulled up or down through the loops of the previous row, in a *knit* or *purl* stitch respectively. Loops appear aligned in columns on the *wale* direction. When the yarn reaches the end of a row, it is typically bent back to form the next row. The first and last row are stitched in a different way to avoid unraveling, while the beginning and end of a yarn are simply tied to the fabric.

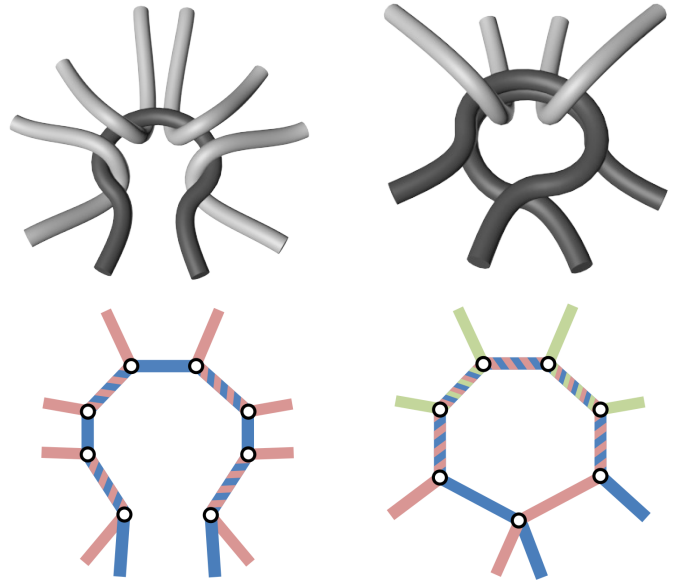


Fig. 3. Close-up examples of complex stitches, showing full 3D views and schematic representations of the corresponding discretizations. Left: an *increase* with two *knit* stitches. Right: a *decrease* with two stacked yarns and a *purl* stitch.

Fig. 2-left shows several loops of a fabric knitted in *stockinette* pattern, which is the simplest pattern, with all knit stitches. Throughout the paper, we also show simulated examples of other simple patterns: *garter*, which alternates rows of knit and purl stitches, and *rib*, which repeats two knit stitches followed by two purl stitches. Kaldor et al. [4] provide an excellent description of how yarns are stitched together to produce a knitted fabric and its behavior. We refer the reader to their paper for representative images of each simple knit pattern.

However, as discussed by Yuksel et al. [24], knitted fabrics allow for very diverse types of stitches, which produce interesting geometric and visual patterns on the overall fabric, and also contribute to diverse macroscopic mechanics. In addition to *knit* and *purl* stitches, we can model:

- *yarn-over* stitches, which lay the yarn without stitching it to the previous row, deliberately creating a hole in the fabric.
- *increases* that combine *knit*, *purl* and *yarn-over* stitches. These are stitched to one single loop of the previous row, effectively increasing the number of stitches in the current row.
- *decreases* using *knit* or *purl* stitches. Several consecutive loops are stacked together and stitched to the next row using a *knit* or a *purl*, effectively reducing the number of stitches in the next row.

Fig. 3 shows close-up examples of some of these stitches. They can be combined to produce very diverse patterns, such as the ones shown in Fig. 4.

Woven and knitted yarns undergo multiple different forces, both internal due to their own deformation, and external due to yarn-yarn contact. The macroscopic mechanical behavior is largely determined by yarn-yarn contact, with three dominating effects: (i) contact at crossings or stitches, (ii) contact between adjacent yarns or loops when

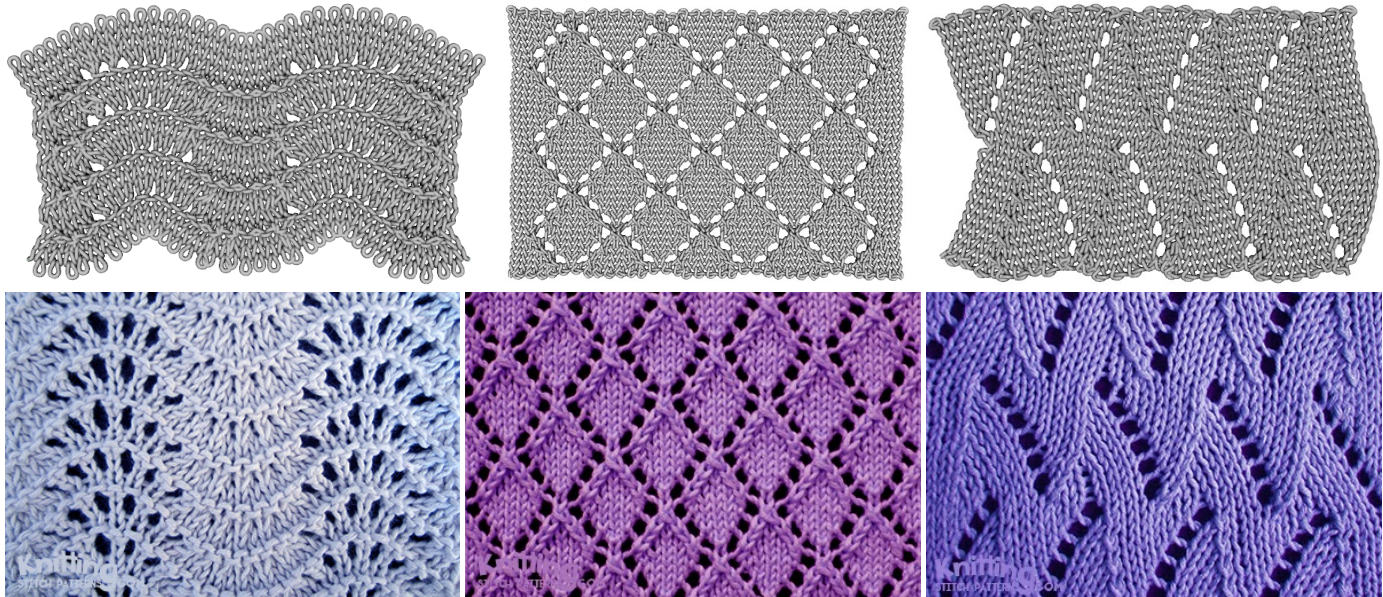


Fig. 4. Three different simulated knitting patterns (top) and their corresponding real photographs (bottom). From left to right: Feather and Fan, Openwork Diamonds, and Flame Chevron. Real photographs courtesy of knittingstitchpatterns.com.

the fabric tightens, and (iii) friction under inter-yarn sliding or shear. The specific sources of macroscopic force effects in woven and knitted cloth are rather different though. Woven cloth is almost inextensible, and its macroscopic shear and bending behavior is dominated by inter-yarn contact forces. In knitted cloth, on the other hand, the geometry of stitches and loops largely affects macroscopic mechanics. Stretch and shear of a knitted garment are dominated first by the bending resistance of yarns as loops deform, then adjacent loops may enter into contact, and finally stretching of the yarns themselves resists additional deformation. When a knitted fabric is laid flat, elastic energy is present due to yarn bending and yarn wrapping. When the fabric is allowed to relax, it will undergo some macroscopic deformation. With a garter pattern, the bending deformation produced by stitch unwrapping is compensated on alternate rows and columns of loops. On a stockinette pattern, rows and columns curl in opposite directions (See Fig. 5-left). On a rib pattern, each pair of stitches curls in opposite direction, leading to a significant compression of the fabric (See Fig. 5-right).

In Section 4, we present force models that capture the essential yarn contact mechanics under our compact yarn representation, and we demonstrate how they reproduce the expected nonlinearity and anisotropy of knitted fabrics.

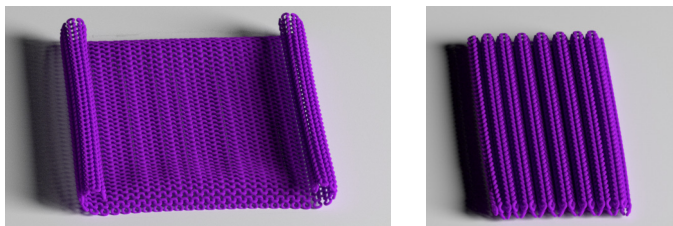


Fig. 5. Curling behavior due to stitch unwrapping. Left: stockinette pattern. Right: rib pattern.

3.2 Discretization Using Contact Nodes

Now we introduce our central idea, the representation of yarn-based fabrics using persistent contacts. Our strategy to discretize yarn-based fabric is to identify the minimum set of persistent yarn-yarn contacts that allow representing all relevant deformation modes. Wherever two or more yarns exhibit a persistent contact, a single 3D point can be used to represent all contacting yarns, thereby eliminating the need to detect and resolve contact.

Each persistent contact node is then augmented with sliding coordinates that allow the yarns to slide tangent to the contact. We generalize the initial two-yarn approach [6] to contact nodes with an arbitrary number of yarns, where each yarn contributes one sliding coordinate to the contact node. In a contact node with n yarns, $\mathbf{q} = (\mathbf{x}, u_1, \dots, u_n)$ constitutes a $(3+n)$ -Degree-of-Freedom (DoF) node, with \mathbf{x} the 3D position of the node, and u_1, \dots, u_n the rest arc lengths of the n yarns in contact, which act as sliding coordinates.

For simulation purposes, we consider the yarn to be formed by straight segments between contact nodes. For rendering purposes, on each contact node we fit a plane to the incident segments using a standard SVD, offset the yarns along the normal of this plane, and interpolate the resulting points using smooth splines. Even high curvature situations, such as the one in Fig. 5-right, exhibit locally sufficiently planar configurations, thanks to the high resolution of the discretization. To move each yarn along the normal, we use reference directions computed at the rest state, taking into account the knitting/weaving pattern.

We follow the framework of Sueda et al. [25] to derive the equations of motion, linearly interpolating kinematic magnitudes along yarn segments and applying the Lagrange-Euler equations. We omit the full derivation here, which differs from the original work for woven cloth [6] only w.r.t. the force model.

3.2.1 Yarn Crossings in Woven Cloth

The persistent-contact strategy can be applied to woven fabrics by placing one persistent contact node at each crossing of warp and weft yarns [6]. Sliding coordinates allow the yarns at a contact node to slide along each other, effectively producing 5-DoF contact nodes.

3.2.2 Two-Yarn Stitches in Knitted Cloth

In a simple stitch, such as a *knit* or a *purl*, a loop from one row is passed through two loops of the previous row. This arrangement produces two stitch contacts, as shown in Fig. 2. During normal operation of the fabric, i.e., unless a stitch is pulled out, the two yarns at each stitch contact are wrapped around each other persistently. Based on this observation, we discretize knitted fabrics by placing two 5-DoF contact nodes at the two end points of each stitch contact, as shown in Fig. 2-right. This discretization captures the most important degrees of freedom in a loop, and allows us to represent any knit pattern based on purl and knit stitches between two yarns. Using a single contact node per stitch contact would miss important loop deformation modes, such as the stretching of fabric due to loop deformation.

In the case of *knit* and/or *purl* stitch configurations, each loop has typically 4 stitch contacts, hence it shares 8 contact nodes with other loops. As a result, a garment with N loops has approximately $4N$ contact nodes and $20N$ DoFs.

In the case of *increases*, a loop can have an arbitrary number of stitches, depending on the number of loops of the next row that are knitted together. However, even though *increases* involve more than two yarns, stitches are always made between exactly two yarns, as in standard *knits* and *purls*. Therefore the discretization remains the same, with two contact nodes per stitch and two sliding coordinates per contact node (one for each yarn).

3.2.3 Stacked Stitches in Knitted Cloth

In the case of *decreases*, two or more loops are stacked together and stitched to the next row, producing stitches with more than two yarns. Our generic contact node discretization can accommodate these additional yarns through contact nodes with an arbitrary number of degrees of freedom. A persistent contact is shared by all the yarns involved in the stitch, and since each yarn contributes one sliding coordinate, a stitch with n yarns effectively produces a compact discretization with two persistent contact nodes, each with $3 + n$ DoFs. Contact forces are computed in a pair-wise manner between yarns actually in contact. As a result, we can conveniently design pairwise force models, as described in Section 4, and use the same force models for persistent contacts involving an arbitrary number of yarns.

It is important to note that this discretization is limited to contact configurations that can be represented by only one set of spatial coordinates: sliding motions must not lead to a splitting of the contact node into two or more nodes. Acceptable configurations boil down to having two groups, each made of an arbitrary number of parallel stacked yarns. Thankfully, *decreases* naturally satisfy this discretization constraint, and remain valid as long as the contact is persistent.

4 FORCE MODEL

We now describe the forces computed on yarn-level fabrics, which include gravity, internal elastic forces of yarns, non-penetration contact forces between yarns, friction, and damping. In our design of the specific force models, we have identified key deformation modes of the yarn structure that suffer resistance. In some cases, particularly for yarn bending, our force model groups the effect of both internal and contact forces. This is a crucial aspect in the design of force models with persistent contacts, because the lack of degrees of freedom in the normal direction of contacts prevents the use of typical penalty potentials or non-penetration constraints.

For gravity, yarn stretch (governed by the Elastic modulus Y), and contact between adjacent loops we use exactly the original formulations for woven cloth [6]; therefore, we refer the reader to the original paper for details. In our force model, we include elastic potentials for two major deformation modes, which we describe first: yarn bending and stitch wrapping.

Next, we introduce a model for the computation of normal compression at inter-yarn contact. We extend the original method for yarn crossings and two-yarn stitches, and we propose a general model that supports stacked stitches with an arbitrary number of yarns. Our model assumes equilibrium conditions in the direction normal to contact, to estimate compression forces in a least-squares manner. Based on such compression forces, we also provide a model of inter-yarn sliding friction for stacked stitches with an arbitrary number of yarns.

We conclude the section with the description of an elastic force for the preservation of the lengths of stitch contacts. For damping, we use the Rayleigh model, although we found that, on very high-resolution fabrics, it is difficult to damp deformations without suffering numerical damping, and it is worth testing other damping models.

According to textile literature [26], the contribution of dynamic yarn twisting is minor, especially compared to dominant forces such as stretch and bending. Therefore, following the general approach, we do not include yarn twist in our force model. Yarn pre-twisting, on the other hand, has an influence on other yarn parameters [27]. We capture this effect by varying bending stiffness and yarn radius accordingly.

The formulations of forces and their Jacobians, except for stitch wrapping, are equivalent to the ones derived for woven cloth [6]. We provide full derivations of forces and Jacobians of stitch wrapping in the Appendix.

4.1 Yarn Bending

Given two consecutive yarn segments, we define an elastic potential based on the angle θ between them:

$$V = k_b \frac{\theta^2}{\Delta u}. \quad (1)$$

Here Δu is the summed arc length of both segments. For small angles, the bending stiffness is due to internal forces during yarn bending, and can be defined as $k_b = B\pi R^2$, with B the bending modulus and R the yarn radius. This is identical to the bending model implemented for woven

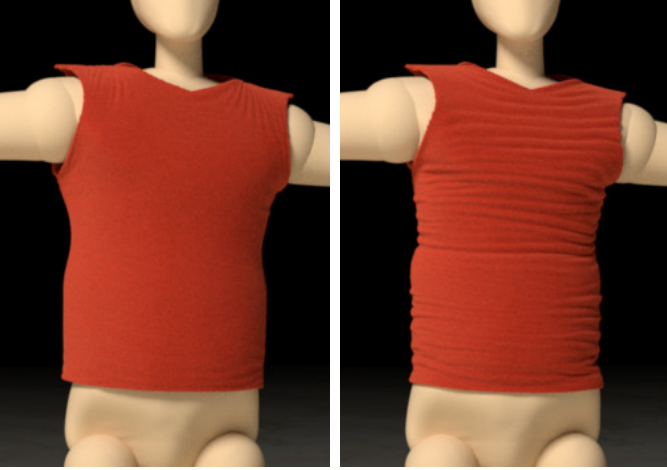


Fig. 6. A knit shirt with (left) and without (right) rest-shape bending compensation. Without compensation, the garment shrinks and exhibits unnatural wrinkles.

cloth [6]. Our bending model differs, however, for large bending angles. Under this situation, the deformation of loops leads to contact between loops of different rows (e.g., the horizontal pink and blue segments in Fig. 2), or *bending jamming*. We model this effect after the shear jamming model in [6], by smoothly increasing the bending stiffness by three orders of magnitude after a certain threshold ($\theta = \pi/2$ in our examples).

To initialize the yarn layout for a knitted garment, we first lay the loops and stitches following an input stitch map. Stitch maps are knitting charts where the resulting fabric has been relaxed to its rest configuration. These charts conveniently provide knitting instructions as well as the post-relaxed shape and position of each loop. Any other input providing similar information could also be used, such as the artist drawing of a pattern or the mesh-based relaxation of Yuksel et al. [24].

The resulting layout, however, may still not be at rest in this initial configuration due to unbalanced bending energies, and the garment may compress and wrinkle when relaxed. In order to compensate for the rest-shape bending, we first relax a small characteristic rectangle of cloth, by simulating it without gravity until it reaches static equilibrium. For complex knits, we choose the smallest rectangle that contains the full knitting pattern. For simpler regular knits, we choose a 5 cm \times 5 cm rectangle, as we found it sufficient to capture characteristic shapes of loops in our examples. After relaxation, we apply the resulting loop shapes in the initialization of the yarn layout for the entire garment. Fig. 6 compares a piece of fabric with and without rest-shape bending compensation. Our bending compensation is not optimal, as it relies on model parameters that are not optimal either. This explains differences between real-world patterns and our simulated patterns in Fig. 4.

4.2 Stitch Wrapping

At each stitch contact, yarn segments are wrapped around each other, as shown in Fig. 2 for two-yarn stitches and in Fig. 3 for stacked stitches. This wrapping produces a deformation energy through contact, which is different from



Fig. 7. Knit garment with a stockinette pattern, with its characteristic curling behavior at the edges.

the twist energy of the individual yarns. Due to our discretization, yarn bending does not capture this deformation, and we therefore require an explicit stitch wrapping energy term. Fig. 8 shows the wrapping in more detail, along with the notation we follow.

We measure the amount of wrapping as the relative angle between opposite yarn segments around the central axis of the stitch contact. For a stacked contact, this is done between every pair of yarns, except for pairs where yarns are parallel to one another. W.l.o.g., we describe the wrapping computations using a two-yarn stitch as example.

Given the two contact nodes of the stitch contact, \mathbf{q}_0 and \mathbf{q}_1 , the unit vector \mathbf{e} between them defines the central axis. We define a wrapping angle ψ between the blue yarn segment from \mathbf{q}_0 to \mathbf{q}_4 and its opposite pink yarn segment from \mathbf{q}_1 to \mathbf{q}_3 , and similarly for the other two segments. Specifically, we compute the angle between the normals of the triangles (shown in light blue and light pink in the figure) formed by such yarn segments and the central axis, which acts as a hinge.

For each pair of opposite yarn segments, we define an elastic potential based on the deviation between the wrapping angle ψ and a rest angle ψ_0 :

$$V = \frac{1}{2} k_w L (\psi - \psi_0)^2, \quad (2)$$

where k_w is an empirically set stiffness, and L is the rest length of the stitch contact. After testing different values for

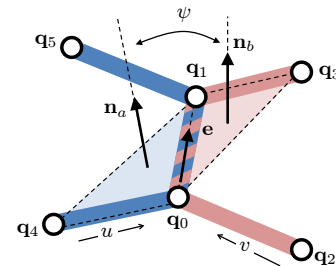


Fig. 8. Representation of a stitch contact. \mathbf{q}_0 and \mathbf{q}_1 are the contact nodes of the stitch contact, with the blue and pink segments belonging to two different loops. We measure stitch wrapping as the angle ψ between the blue and pink triangles, with the central axis \mathbf{e} acting as a hinge.

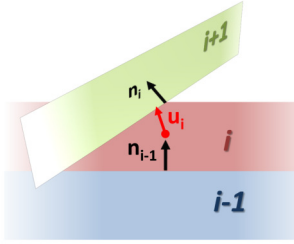
ψ_0 , we chose $\pi/2$ for a visually realistic wrapping effect.

The yarn segments at stitch contacts have the natural tendency to unwrap. In the garter pattern, adjacent rows of loops unwrap in opposite directions. However, in the stockinette pattern, where they unwrap in the same direction, a characteristic behavior emerges: the fabric has a tendency to curl both in wale and course directions. This effect is particularly noticeable at the boundaries of the fabric, as shown in Fig. 5-left and Fig. 7. In the rib pattern, on the other hand, each pair of stitches curls in opposite direction, leading to a natural compression of the fabric, as shown in Fig. 5-right.

4.3 Yarn Contact Compression

The ability to model inter-yarn sliding with friction forces is one of the cornerstones of our method. According to Coulomb's model, friction force is limited by the amount of normal compression at inter-yarn contact. However, due to the lack of degrees of freedom normal to inter-yarn contact, we cannot define a compression potential. We propose an approach to estimate inter-yarn compression forces where we ignore dynamics in the normal direction and assume equilibrium conditions. For a stacked contact, we do this in a least-squares fashion for all yarns together.

Let us assume a contact node with n stacked yarns and $n - 1$ pairwise contacts. The figure on the side shows an example with 3 of these yarns. For yarns i and $i + 1$, we compute a normal vector \mathbf{n}_i pointing from yarn i to $i + 1$, by fitting a plane to the contact node and the adjacent



nodes along the two yarns. The normal force from yarn i to yarn $i + 1$ is $\lambda_i \mathbf{n}_i$, with a non-sticking constraint $\lambda_i \geq 0$.

For each stacked yarn, we define a compression direction \mathbf{u} as the average of its two contact normals. Then, given the two compressive forces acting on a stacked yarn, together with all other forces \mathbf{F}_i acting on the yarn, we express a net force f_i along the compression direction:

$$f_i = \mathbf{u}_i^T (\mathbf{F}_i + \lambda_{i-1} \mathbf{n}_{i-1} - \lambda_i \mathbf{n}_i). \quad (3)$$

For the first and last yarns in a stacked contact, there is only one compressive force. For woven cloth, in \mathbf{F}_i we sum up stretch and bending forces of yarn i on the contact node. For knitted cloth, we also add stitch wrapping forces. Due to yarn volume, the central axes of yarns in contact are separated by a certain distance, which is not present in our model. In woven fabric, this distance is called *crimp*. This distance produces a misalignment of stretch forces even in planar configurations. To correctly estimate the normal force due to stretch, we offset nodes along the contact normal.

To compute the normal forces λ , we perform a least-squares minimization of net compressive forces, i.e., $\lambda = \arg \min \frac{1}{2} \mathbf{f}^T \mathbf{f}$, subject to non-sticking constraints $\lambda \geq 0$. We can write the vector of net compressive forces \mathbf{f} as a linear expression of normal forces, $\mathbf{f} = \mathbf{A} \lambda + \mathbf{b}$, stacking expression (3) for all yarns in contact. We solve the minimization

using the Lagrange multipliers method, which leads to the solution

$$\lambda = (\mathbf{A}^T \mathbf{A})^{-1} \cdot \max(0, -\mathbf{A}^T \mathbf{b}). \quad (4)$$

We reach a compact closed-form expression of normal forces amenable to efficient GPU implementation. For just two yarns in contact, the method reduces to the solution described in [6] for simple woven cloth.

4.4 Sliding Friction

We model Coulomb friction on sliding coordinates using anchored springs, as we did earlier for simple woven and knitted cloth.

In the case of stacked contact nodes, we make a distinction between pairs of yarns with the same sliding direction (yarns with parallel stacking) and pairs of yarns with two different sliding directions (yarns with non-parallel stacking). For non-parallel stacked yarns, friction is modeled using anchored springs on each yarn's sliding coordinate independently [6]. For parallel stacked yarns, however, frictional contact is influenced by both yarns, since both are constrained to slide along the same axis. Therefore, the sliding degrees of freedom of both yarns must be involved in frictional contact computations.

For parallel contact i within the stack, involving yarns i and $i + 1$, we use an anchored spring spanning both yarns, with length $\Delta u^i = u_i - u_{i+1}$ and rest length $\Delta \bar{u}^i = \bar{u}_i^i - \bar{u}_{i+1}^i$. The resulting friction force F^i due to contact i is:

$$F_{u_i}^i = -F_{u_{i+1}}^i = \begin{cases} -k_f (\Delta u^i - \Delta \bar{u}^i), & \text{if stick} \\ -\text{sign}(\Delta u^i - \Delta \bar{u}^i) \mu \lambda_i, & \text{if slip,} \end{cases} \quad (5)$$

where μ is the friction coefficient and λ_i is the compression force for contact i within the stacking as computed in Section 4.3. During dynamic friction, we adjust each anchor point according to the deviation of the corresponding sliding coordinate from its maximal stick position.

4.5 Length of Stitch Contacts

When the end node of one stitch contact slides, the other node should slide too to preserve the material length of the contact stitch and avoid artificial creation or deletion of material. We assume that the material length of stitch contacts remains constant, and we enforce this using a penalty energy. For a stitch contact between nodes \mathbf{q}_0 and \mathbf{q}_1 as shown in Fig. 8, with arc length $l = u_1 - u_0$ and rest length L , we define the energy as:

$$V = \frac{1}{2} k_l L \left(\frac{l}{L} - 1 \right)^2, \quad (6)$$

where k_l is the stiffness of the length constraint.

Yarn sliding is negligible under small forces, because friction keeps the yarns in place. However, sliding may indeed take place under moderate forces, such as extensive stretch. In that case, sliding produces plastic deformations that remain when forces are released. Fig. 9 shows an example where a small piece of fabric (left) is overly stretched to the point where yarns slide (middle), and plastic deformation is present when the fabric is released (right).

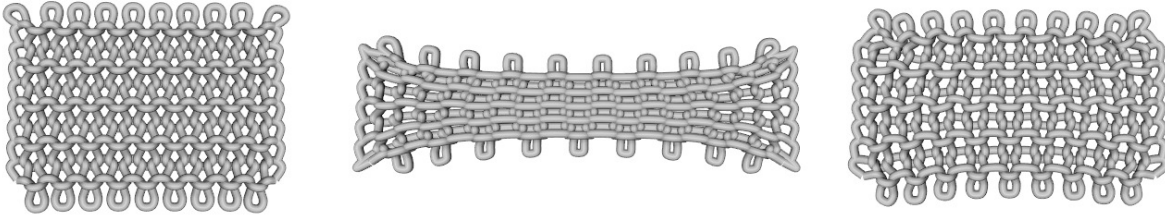


Fig. 9. A small piece of fabric (left) is overly stretched to the point where inter-yarn friction cannot prevent yarn sliding (middle), and plastic deformations are evident when forces are released and the fabric goes back to rest (right).

Example	Loop width (mm)	Yarn radius R (mm)	Elastic mod. Y (Pa)	Bend. mod. B (Pa)	Wrap mod. k_w (Pa)	Sliding Fric. Coef. μ	Rayleigh damping (α, β)
Sweater (Fig. 1)	3	0.75	1e7	1e-3	1e-2	0.3	10, 0.01
Sleeveless Shirt (Fig. 10)	1	0.25	1e7	3e-4	1e-2	0.3	2, 0.1
Sleeveless Pullover (Fig. 7)	6	1.5	1e7	3e-4	1e-2	0.3	5, 0.01

TABLE 1
Parameter values used in our examples.

5 RESULTS

We have integrated our model in the implicit-integration algorithm proposed in [6]. For simple knits, the regularity of the patterns produces a sparse system matrix with at most 11 non-zero 5x5 blocks per block-row. We handle blocks produced by collisions and seams in a tail matrix. All our examples were executed on a 3.4 GHz Quad-core Intel Core i7-3770 CPU with 32GB of memory, with an NVIDIA Tesla K40 graphics card with 12GB of memory. Simulations were executed with a time step of 1ms, and the parameter values used in the large-scale examples are listed in Table 1. Please see our accompanying video for all animation results.

5.1 High-Resolution Examples

5.1.1 Sweater

We dressed a dancing female mannequin (Fig. 1) with a sweater made of 56K loops (224353 stitch contact nodes). The sweater is knit in Garter style, with seams on the sides of the body, the shoulders, the sleeve-body junctions, and along the sleeves. In the textile industry, stitch density is measured as the number of stitches per inch, and is called Gauge (GG). Our sweater has 6.5 stitches per inch, a gauge commonly found in real sweaters. The simulation took 96 seconds per visual frame (at 30fps), roughly 7x faster than the approach by Kaldor et al. [5] for a model of similar characteristics (without accounting for hardware differences).

5.1.2 Sleeveless T-shirt

We used a sleeveless T-shirt model to dress a male mannequin performing highly dynamic karate motions (Fig. 10). The T-shirt has 325K loops (1.25M stitch contact nodes), 20 stitches per inch, and is knit in Garter style. This gauge (20 GG) is commonly found in off-the-shelf T-shirts made of carded cotton. The simulation took an average of 7.4 minutes per visual frame (at 30fps), showing how garments with life-like resolutions can be computed in tractable time with our approach.

5.2 Macroscopic Nonlinearities

5.2.1 Weaving/Knitting Pattern Comparisons

We replicated several well-known knitting patterns involving two-yarn and stacked stitches and simulated them using our model. Figure Fig. 5 compares the *Feather and Fan*, the *Openwork Diamonds* and the *Flame Chevron* simulated patterns to real photographs. We can observe how the fabric naturally realizes the complex shapes prescribed by each particular sequence of stitches.

In addition, we compared the dynamics of a wider range of samples to highlight how yarn-level dynamics affect the macroscopic behavior of fabric. Besides the aforementioned knitted patterns, we also simulated two standard knitted patterns (garter and rib), and a standard woven pattern (plain). All samples use yarns with 1mm radius with the exact same parameters. The samples are dropped onto a sphere and are simulated until coming to a rest, as shown in Fig. 12.

5.2.2 Stockinette Curl

The stockinette pattern produces a curl behavior in the fabric, and in our model this effect is captured by the stitch wrapping forces introduced in Section 4.2. We show the effect of curl in a stockinette garment in Fig. 7. The garment is a sleeveless wool pullover, with 8750 loops (34416 stitch contact nodes). As in real cloth, the curl effect is particularly visible at the edges of the fabric. Here, the lower edge and the collar wrap around themselves.

5.2.3 Rib Stretch Nonlinearities

One of the main advantages of yarn-level models is the ability to naturally capture complex nonlinear deformations. Fig. 11 shows an example nonlinear behavior observed when stretching a piece of rib fabric, which appears compressed at rest, and with the characteristic ridges of the rib pattern. The plot shows the force applied to one side of the fabric vs. the side-to-side distance, and highlights the existence of 3 regimes during the deformation. First, the ridges are flattened, and stretch is opposed mainly by stitch wrapping forces. Second, the loops are deformed, and



Fig. 10. Simulation of a high-resolution shirt with 325K loops (1.25M contact nodes, 6.25M DoFs), computed at 7.4 minutes per frame.

stretch is opposed mainly by yarn bending. And third, the yarns themselves are stretched. The nonlinear stretch behavior emerges naturally when using our yarn-level model thanks to the low-level structural representation and force models, but is difficult to capture using traditional mesh-based approaches.

5.2.4 Yarn Pullout

The sliding coordinates allow rich and complex non-linear effects through plastic deformation. We take a garter fabric, fix its boundaries except on one row, and pull on the yarn that makes the row. To dynamically adapt the persistent contacts, we collapse very small segments, and eventually break the required contacts by turning 5-DoF nodes into two 3-DoF nodes (one for each yarn). As shown in Fig. 13, the fabric deforms and separates as the yarn slides through the loops, unraveling the stitches. This effect is different from tearing since yarns remain intact, and only the structure of the yarn-level cloth is affected. Producing this type of deformation using a mesh-based cloth model would be very complex, but it is easy and natural with our yarn-level model.

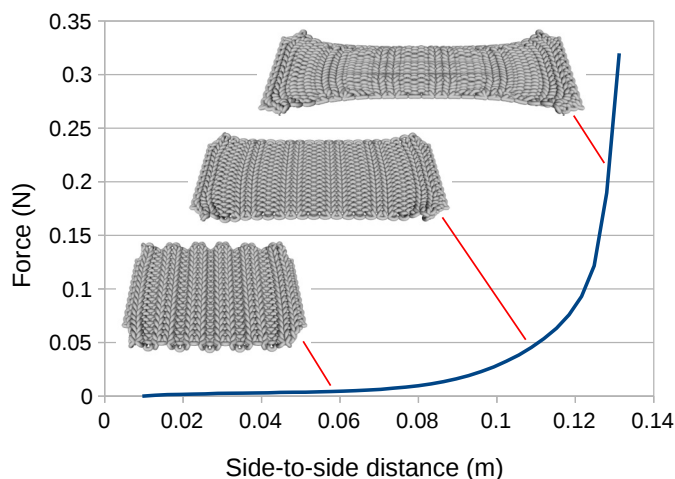


Fig. 11. Force plot of a stretched rib fabric. The highly nonlinear behavior is evident, with three different regimes corresponding mainly to opposing wrapping, bending and stretching forces.

6 CONCLUSIONS AND FUTURE WORK

In this paper, we have presented an efficient method to simulate cloth at the yarn level. We based our method on an efficient representation of knitted cloth that treats yarn-yarn contacts as persistent, thereby avoiding expensive contact handling altogether. We generalized this representation to model complex knitted cloth stitches involving multiple stitches per loop as well as stacked yarns. Our compact discretization allows us to capture the relevant yarn-level deformation modes, achieving complex, nonlinear and plastic effects at a macroscopic scale.

Although our persistent contact model can accommodate a wide variety of patterns, there are some notable patterns where yarns cannot be assumed to be in a persistent contact state. An example of such a configuration are cables, where one group of stitches is crossed over another, creating interesting relief effects. In this case, contact handling would be a particular case of self-collision handling, where contact regions remain almost fixed.

Persistent contacts also ignore three aspects of yarn-yarn contact:

- Yarn compliance. However, yarn stiffness in the transverse direction is very high, and the effect of compliance is minimal. Ignoring this compliance plays in our advantage, as we avoid the need to solve very stiff equations.
- The effect of inertial forces on friction. This effect might translate into milder friction under high accelerations, but it can be compensated by slightly increasing the coefficient of friction.
- Inter-yarn separation. Stitches may get loose under cloth compression. In this case, we do not let yarns separate, but this separation is minimal due to the interleaved structure of the fabric. At the same time, we correctly ignore friction forces.

In addition, our model omits twist, following observations from the textile literature, and our results seem to validate that it does not contribute to the main macroscopic effects. However, it would be interesting to analyze its actual effect, both in pre-twisted yarn assemblies, as well as during deformations that induce dynamic twist.

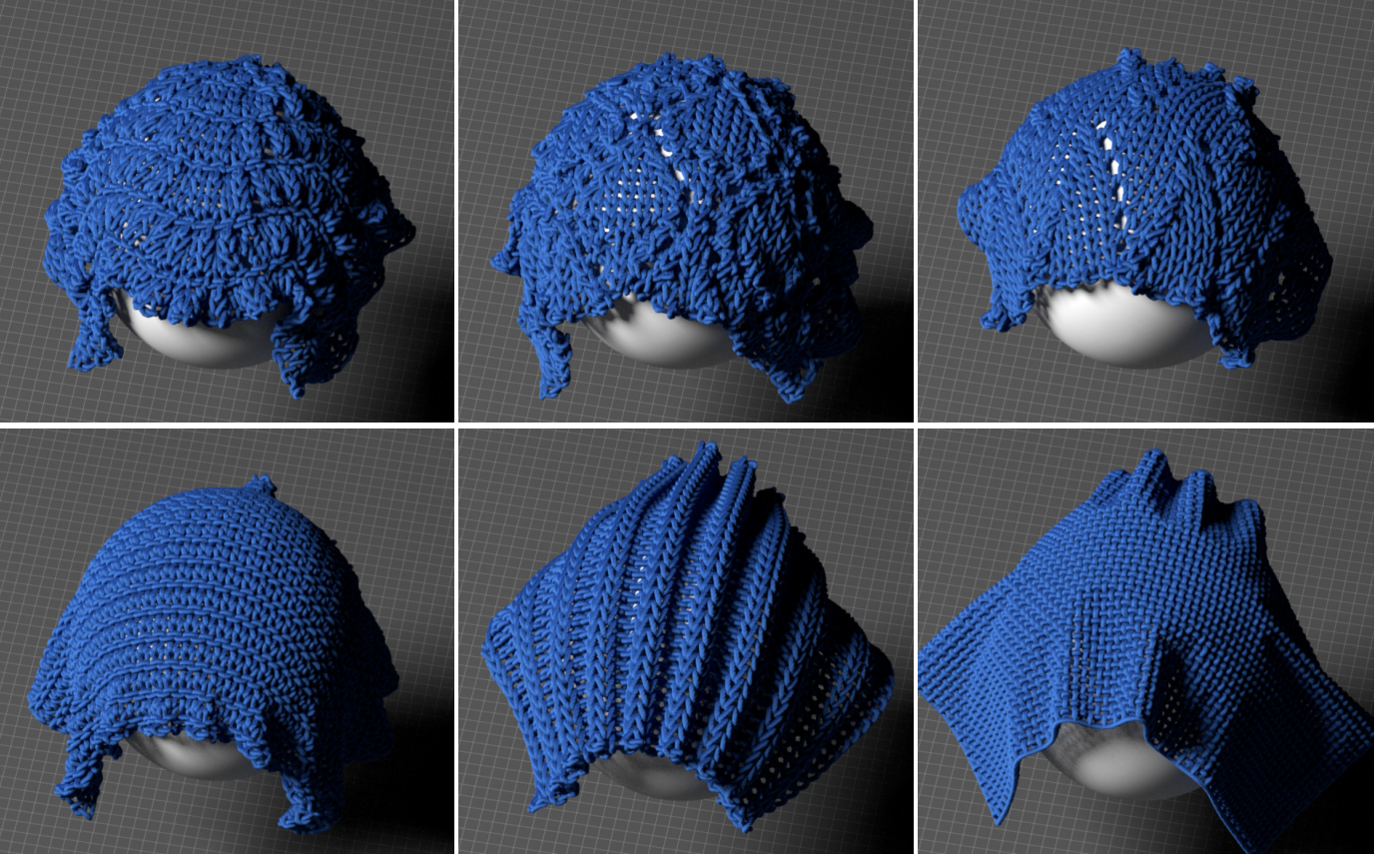


Fig. 12. Six different yarn-level cloth patterns with different macroscopic behaviors. Top row, from left to right: knitted Feather and Fan, knitted Openwork Diamonds and knitted Flame Chevron. Bottom row, from left to right: knitted Garter, knitted Rib and plain woven.

Finally, in our examples, model parameters are artist-tuned. In future work, we would like to estimate these parameters from example deformations, or derive them from more complex simulations with contact mechanics and physically based parameters. This would also enable a direct comparison to models with full yarn-yarn contact.

APPENDIX STITCH WRAPPING FORCES AND JACOBIANS

The central axis of the stitch is defined by a vector

$$\mathbf{e} = \frac{\mathbf{x}_1 - \mathbf{x}_0}{\|\mathbf{x}_1 - \mathbf{x}_0\|}, \quad (7)$$

with derivatives

$$\frac{\partial \mathbf{e}}{\partial \mathbf{x}_0} = -\frac{1}{\|\mathbf{x}_1 - \mathbf{x}_0\|} (\mathbf{I} - \mathbf{e} \mathbf{e}^T) \quad \text{and} \quad \frac{\partial \mathbf{e}}{\partial \mathbf{x}_1} = -\frac{\partial \mathbf{e}}{\partial \mathbf{x}_0}. \quad (8)$$

The triangles $(\mathbf{q}_0, \mathbf{q}_1, \mathbf{q}_4)$ and $(\mathbf{q}_0, \mathbf{q}_3, \mathbf{q}_1)$ have normal vectors

$$\mathbf{n}_a = \frac{\mathbf{v}_a}{\|\mathbf{v}_a\|}, \quad \text{with } \mathbf{v}_a = (\mathbf{x}_4 - \mathbf{x}_1) \times (\mathbf{x}_0 - \mathbf{x}_1). \quad (9)$$

$$\mathbf{n}_b = \frac{\mathbf{v}_b}{\|\mathbf{v}_b\|}, \quad \text{with } \mathbf{v}_b = (\mathbf{x}_0 - \mathbf{x}_1) \times (\mathbf{x}_3 - \mathbf{x}_1). \quad (10)$$

It is convenient to define the auxiliary vectors

$$\mathbf{x}_{a0} = \mathbf{x}_4 - \mathbf{x}_1, \quad \mathbf{x}_{a1} = \mathbf{x}_0 - \mathbf{x}_4, \quad \text{and} \quad \mathbf{x}_{a4} = \mathbf{x}_1 - \mathbf{x}_0. \quad (11)$$

$$\mathbf{x}_{b0} = \mathbf{x}_1 - \mathbf{x}_3, \quad \mathbf{x}_{b1} = \mathbf{x}_3 - \mathbf{x}_0, \quad \text{and} \quad \mathbf{x}_{b3} = \mathbf{x}_0 - \mathbf{x}_1. \quad (12)$$

Their derivatives, $\frac{\partial \mathbf{x}_{ai}}{\partial \mathbf{x}_j}$ and $\frac{\partial \mathbf{x}_{bi}}{\partial \mathbf{x}_j}$, can take the values $\{\mathbf{I}, -\mathbf{I}, \mathbf{0}\}$.

The wrapping angle between the triangles is

$$\psi = \arccos(\mathbf{n}_a^T \mathbf{n}_b), \quad (13)$$

and its derivatives take the form

$$\frac{\partial \psi}{\partial \mathbf{x}_i} = \frac{1}{\|\mathbf{v}_b\|} \mathbf{n}_b^T \mathbf{e}^T \mathbf{x}_{bi} - \frac{1}{\|\mathbf{v}_a\|} \mathbf{n}_a^T \mathbf{e}^T \mathbf{x}_{ai}. \quad (14)$$

From the potential energy in (2), forces on contact nodes ($i \in \{0, 1, 3, 4\}$) are computed as:

$$\mathbf{F}_{\mathbf{x}_i} = -k_w L (\psi - \psi_0) \left(\frac{\mathbf{x}_{bi}^T}{\|\mathbf{v}_b\|} \mathbf{e} \mathbf{n}_b - \frac{\mathbf{x}_{ai}^T}{\|\mathbf{v}_a\|} \mathbf{e} \mathbf{n}_a \right). \quad (15)$$

And their Jacobians take the form:

$$\begin{aligned} \frac{\partial \mathbf{F}_{\mathbf{x}_i}}{\partial \mathbf{x}_j} = & -k_w L \left(\frac{\mathbf{x}_{bi}^T}{\|\mathbf{v}_b\|} \mathbf{e} \mathbf{n}_b - \frac{\mathbf{x}_{ai}^T}{\|\mathbf{v}_a\|} \mathbf{e} \mathbf{n}_a \right) \left(\frac{\mathbf{x}_{bj}^T}{\|\mathbf{v}_b\|} \mathbf{e} \mathbf{n}_b - \frac{\mathbf{x}_{aj}^T}{\|\mathbf{v}_a\|} \mathbf{e} \mathbf{n}_a \right)^T \\ & - \frac{k_w L (\psi - \psi_0)}{\|\mathbf{v}_b\|} \left(\frac{\mathbf{x}_{bi}^T}{\|\mathbf{v}_b\|} \mathbf{e} (\mathbf{I} - 2 \mathbf{n}_b \mathbf{n}_b^T) \mathbf{x}_{bj}^* + \mathbf{n}_b \mathbf{x}_{bi}^T \frac{\partial \mathbf{e}}{\partial \mathbf{x}_j} + \mathbf{n}_b \mathbf{e}^T \frac{\partial \mathbf{x}_{bi}}{\partial \mathbf{x}_j} \right) \\ & + \frac{k_w L (\psi - \psi_0)}{\|\mathbf{v}_a\|} \left(\frac{\mathbf{x}_{ai}^T}{\|\mathbf{v}_a\|} \mathbf{e} (\mathbf{I} - 2 \mathbf{n}_a \mathbf{n}_a^T) \mathbf{x}_{aj}^* + \mathbf{n}_a \mathbf{x}_{ai}^T \frac{\partial \mathbf{e}}{\partial \mathbf{x}_j} + \mathbf{n}_a \mathbf{e}^T \frac{\partial \mathbf{x}_{ai}}{\partial \mathbf{x}_j} \right), \end{aligned} \quad (16)$$

where \mathbf{u}^* denotes the cross product matrix for vector \mathbf{u} .

ACKNOWLEDGMENTS

We wish to thank Jaime González, Eder Miguel, Jesús Pérez, Sophie Boichet and the GMRV group for diverse help with our submission, Wenzel Jacob for support with Mitsuba, and

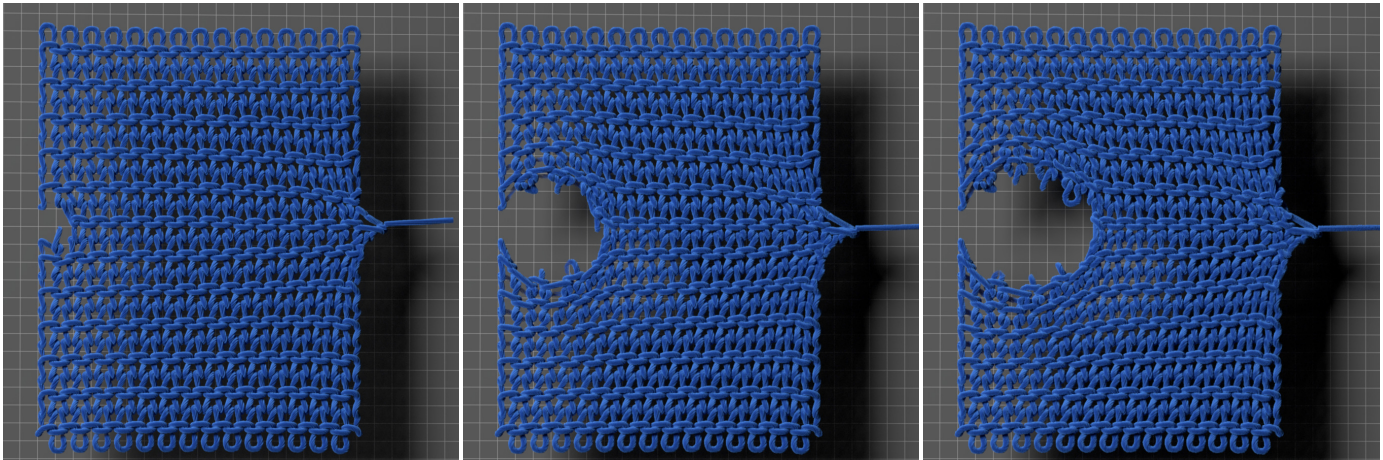


Fig. 13. Yarn pullout. A single row is pulled out of the fabric, unraveling the stitches and creating complex non-linear plastic effects.

the Berkeley Garment Library [28] for the mannequin model and animations. This work was supported in part by the Spanish Ministry of Economy (TIN2012-35840 and TIN2015-70799-R) and the European Research Council (ERC-2011-StG-280135 Animetrics). The work of Gabriel Cirio and Jorge Lopez-Moreno was funded by the Spanish Ministry of Science and Education through Juan de la Cierva Fellowships.

REFERENCES

- [1] O. Etmuss, M. Keckeisen, and W. Strasser, "A fast finite element solution for cloth modelling," in *Computer Graphics and Applications, 2003. Proceedings. 11th Pacific Conference on*, 2003, pp. 244–251.
- [2] D. E. Breen, D. H. House, and M. J. Wozny, "Predicting the drape of woven cloth using interacting particles," in *Proceedings of the 21st Annual Conference on Computer Graphics and Interactive Techniques*, ser. SIGGRAPH '94. New York, NY, USA: ACM, 1994, pp. 365–372. [Online]. Available: <http://doi.acm.org/10.1145/192161.192259>
- [3] X. Provot, "Deformation constraints in a mass-spring model to describe rigid cloth behavior," in *In Graphics Interface*, 1995, pp. 147–154.
- [4] J. M. Kaldor, D. L. James, and S. Marschner, "Simulating knitted cloth at the yarn level," *ACM Trans. Graph.*, vol. 27, no. 3, p. 65:165:9, 2008.
- [5] J. M. Kaldor, D. L. James, and S. Marschner, "Efficient yarn-based cloth with adaptive contact linearization," *ACM Transactions on Graphics*, vol. 29, no. 4, pp. 105:1–105:10, jul 2010.
- [6] G. Cirio, J. Lopez-Moreno, D. Miraut, and M. A. Otaduy, "Yarn-level simulation of woven cloth," *ACM Trans. Graph.*, vol. 33, no. 6, pp. 207:1–207:11, Nov. 2014.
- [7] G. Cirio, J. Lopez-Moreno, and M. A. Otaduy, "Efficient simulation of knitted cloth using persistent contacts," in *Proceedings of the 14th ACM SIGGRAPH / Eurographics Symposium on Computer Animation*, ser. SCA '15. ACM, 2015, pp. 55–61.
- [8] F. T. Peirce, "The geometry of cloth structure," *Journal of the Textile Institute Transactions*, vol. 28, no. 3, pp. T45–T96, 1937.
- [9] J. W. S. Hearle, P. Grosberg, and S. Backer, *Structural Mechanics of Fibers, Yarns, and Fabrics*. New York: John Wiley & Sons Inc, 1969, vol. 1.
- [10] S. Kawabata, M. Niwa, and H. Kawai, "The finite-deformation theory of plain-weave fabrics part i: The biaxial-deformation theory," *Journal of the Textile Institute*, vol. 64, no. 1, pp. 21–46, 1973.
- [11] S.-P. Ng, P.-C. Tse, and K.-J. Lau, "Numerical and experimental determination of in-plane elastic properties of 2/2 twill weave fabric composites," *Composites Part B: Engineering*, vol. 29, no. 6, pp. 735–744, 1998.
- [12] J. Page and J. Wang, "Prediction of shear force and an analysis of yarn slippage for a plain-weave carbon fabric in a bias extension state," *Composites Science and Technology*, vol. 60, no. 7, pp. 977 – 986, 2000.
- [13] Y. Duan, M. Keefe, T. A. Bogetti, and B. Powers, "Finite element modeling of transverse impact on a ballistic fabric," *International Journal of Mechanical Sciences*, vol. 48, no. 1, pp. 33–43, 2006.
- [14] B. Nadler, P. Papadopoulos, and D. J. Steigmann, "Multiscale constitutive modeling and numerical simulation of fabric material," *International Journal of Solids and Structures*, vol. 43, no. 2, pp. 206 – 221, 2006.
- [15] S. Reese, "Anisotropic elastoplastic material behavior in fabric structures," in *IUTAM Symposium on Computational Mechanics of Solid Materials at Large Strains*, ser. Solid Mechanics and Its Applications, C. Miehe, Ed. Springer Netherlands, 2003, no. 108, pp. 201–210.
- [16] M. A. McGlockton, B. N. Cox, and R. M. McMeeking, "A binary model of textile composites: III high failure strain and work of fracture in 3D weaves," *Journal of the Mechanics and Physics of Solids*, vol. 51, no. 8, pp. 1573–1600, 2003.
- [17] Y. Remion, J.-M. Nourrit, and D. Gillard, "Dynamic animation of spline like objects," in *Winter School in Computer Graphics and Visualization*, 1999, pp. 426–432.
- [18] W. Renkens and Y. Kyosev, "Geometry modelling of warp knitted fabrics with 3d form," *Textile Research Journal*, vol. 81, no. 4, pp. 437–443, 2011.
- [19] Y. Jiang and X. Chen, "Geometric and algebraic algorithms for modelling yarn in woven fabrics," *Journal of the Textile Institute*, vol. 96, no. 4, pp. 237–245, 2005.
- [20] O. Nocent, J.-M. Nourrit, and Y. Remion, "Towards mechanical level of detail for knitwear simulation," in *Winter School in Computer Graphics and Visualization*, 2001, pp. 252–259.
- [21] M. J. King, P. Jearanaisilawong, and S. Socrate, "A continuum constitutive model for the mechanical behavior of woven fabrics," *International Journal of Solids and Structures*, vol. 42, no. 13, pp. 3867–3896, 2005.
- [22] W. Xia and B. Nadler, "Three-scale modeling and numerical simulations of fabric materials," *International Journal of Engineering Science*, vol. 49, no. 3, pp. 229–239, 2011.
- [23] E. M. Parsons, M. J. King, and S. Socrate, "Modeling yarn slip in woven fabric at the continuum level: Simulations of ballistic impact," *Journal of the Mechanics and Physics of Solids*, vol. 61, no. 1, pp. 265–292, 2013.
- [24] C. Yuksel, J. M. Kaldor, D. L. James, and S. Marschner, "Stitch meshes for modeling knitted clothing with yarn-level detail," *ACM Trans. Graph.*, vol. 31, no. 4, pp. 37:1–37:12, 2012.
- [25] S. Sueda, G. L. Jones, D. I. W. Levin, and D. K. Pai, "Large-scale dynamic simulation of highly constrained strands," *ACM Trans. Graph.*, vol. 30, no. 4, pp. 39:1–39:10, 2011.
- [26] M. Duhovic and D. Bhattacharyya, "Simulating the deformation mechanisms of knitted fabric composites," *Composites Part A: Applied Science and Manufacturing*, vol. 37, no. 11, 2006.
- [27] N. Pan and D. Brookstein, "Physical properties of twisted structures. ii. industrial yarns, cords, and ropes," *Journal of Applied Polymer Science*, vol. 83, no. 3, pp. 610–630, 2002.
- [28] J. de Joya, R. Narain, J. O'Brien, A. Samii, and V. Zordan, "Berkeley garment library," <http://graphics.berkeley.edu/resources/GarmentLibrary/>.